5 The Acoustic/Elastic Transfer Function and the Sound Reception Process

5.1 Wave Processes and Sound Reception

The last Chapter showed how to characterize the relationship between the Thévenin equivalent driving voltage of the pulser and the output force, $F_t(\omega)$, at the face of the transmitting transducer. That output force will launch waves from the transducer, waves that will propagate and interact with the component being inspected as well as with whatever flaws may be present. A portion of these waves will be captured by a receiving transducer as shown in Fig. 5.1. The waves incident on the receiving transducer will generate a force on that transducer, labeled $F_B(\omega)$ in Fig. 5.1. All the acoustic/elastic wave propagation and scattering interactions that occur between the transmitting transducer and the receiving transducer are complex 3-D wave phenomena.

Later Chapters will describe in detail how models can describe these waves. Here, we are interested in characterizing the role that the acoustic/elastic interactions play in the overall ultrasonic measurement system and we will give some simple examples of those interactions. We will also describe models for characterizing the entire reception process (see Fig. 5.2) where the force, $F_B(\omega)$, is converted into electrical energy at the receiving transducer, transmitted by a cable to the receiver, and then amplified to generate a final system output voltage, $V_R(\omega)$. Like the process of sound generation both the acoustic/elastic process and the reception process can be modeled as transfer functions. The acoustic/elastic transfer function is defined as:

$$t_A(\omega) = \frac{F_B(\omega)}{F_t(\omega)} \tag{5.1}$$

and the reception process transfer function is defined as:

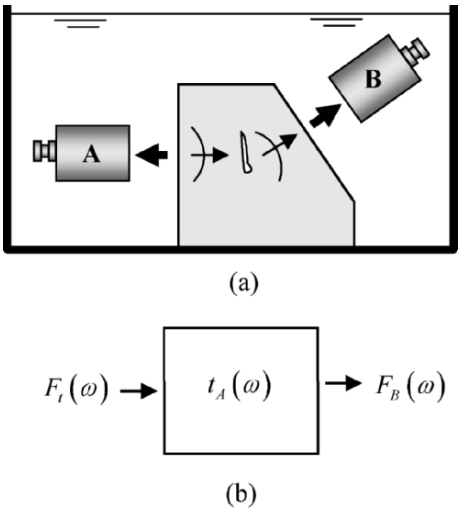

Fig. 5.1. (a) An ultrasonic pitch-catch immersion inspection, showing the acoustic/elastic waves present between the sending transducer and the receiving transducer, and **(b)** an LTI system model of those acoustic/elastic processes whose transfer function is $t_A(\omega)$.

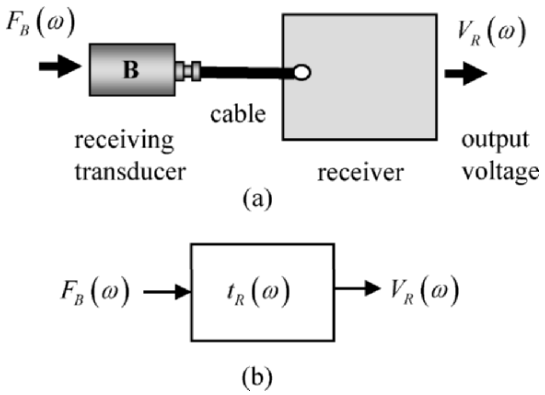

Fig. 5.2. (a) The elements of the reception process – the receiving transducer, the cabling, and the receiver portion of a pulser/receiver, and **(b)** an LTI system model of the reception process whose transfer function is $t_R(\omega)$.

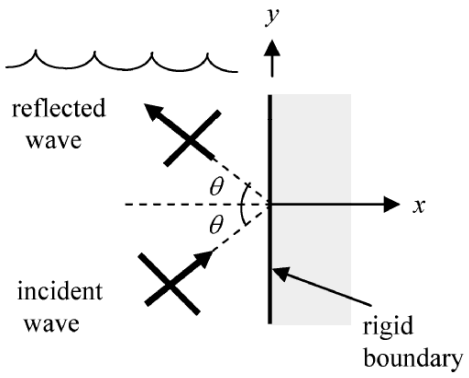

Fig. 5.3. Modeling the interaction of the waves incident on a "blocked" receiving transducer where the waves are treated as plane waves and the transducer surface is treated as a infinite, planar and rigid (immobile) boundary.

$$t_R(\omega) = \frac{V_R(\omega)}{F_B(\omega)} \tag{5.2}$$

5.2 The Blocked Force

The force, $F_B(\omega)$, appearing in both Eqs. (5.1) and (5.2) is a particular force acting on the receiving transducer called the *blocked force*. This blocked force is defined as the force that would be exerted on the receiving transducer if its face was held rigidly fixed (immobile). We will see shortly why this specific force arises naturally when we discuss the reception process. However, we can use a simple model to gain some additional understanding of this force. Consider, for example, the waves incident on a receiving transducer in an immersion setup. Let θ be the angle that these incident waves make with the normal to the transducer and assume that these incident waves behave like harmonic plane waves, as shown in Fig. 5.3. If we neglect any wave diffraction effects at the edges of the receiving transducer, we can model the face of that transducer, when its face is held rigidly fixed, as an infinite plane rigid surface, as shown in Fig. 5.3. The pressure of the incident plane wave can be given as

$$p_{inc} = P_i \exp\left[ik\left(x\cos\theta + y\sin\theta\right) - i\omega t\right] \tag{5.3}$$

and the pressure in the plane reflected wave given by

$$p_{reflt} = P_r \exp\left[ik\left(-x\cos\theta + y\sin\theta\right) - i\omega t \right] \tag{5.4}$$

since it reflects from the surface with the same angle as the incident wave as shown in Appendix D. At the transducer face, $x = 0$, which is held rigidly fixed, the total displacement and velocity normal to the transducer (in the x-direction) must be zero. Thus, from the equation of motion (see Appendix D) we have at the transducer face

$$v_x\left(x,y,t\right)\Big|_{x=0} = \frac{1}{i\omega\rho}\frac{\partial p\left(x,y,t\right)}{\partial x}\bigg|_{x=0} = 0 \tag{5.5}$$

where $p = p_{inc} + p_{reflt}$ is the total pressure. Placing Eqs. (5.3) and (5.4) into Eq. (5.5) we find

$$\frac{ik\cos\theta}{i\omega\rho}\left(P_i - P_r\right)\exp\left(iky\sin\theta - i\omega t\right) = 0 \tag{5.6}$$

so that $P_i = P_r$ and the total pressure, p_B, at the blocked transducer face is just $p_B = 2p_{inc}$. If we let S be the area of the face of the transducer then we see that the blocked force acting on the face of the transducer, $F_B\left(\omega\right) = \iint_S p_B dS$, is just twice that of the force $F_{inc} = \iint_S p_{inc} dS$, exerted by the incident wave over the same area, i.e.

$$F_B\left(\omega\right) = 2F_{inc}\left(\omega\right) \tag{5.7}$$

To summarize: If we assume plane wave interactions at the receiving transducer, the blocked force, $F_B\left(\omega\right)$, is just twice the force, $F_{inc}\left(\omega\right)$, exerted by the waves incident on the area of the receiver. The force, $F_{inc}\left(\omega\right)$, acting on S is computed from the incident waves *as if the transducer were absent*.

Many authors use Eq. (5.7) without further discussion since the plane wave interaction assumption on which it is based is likely a good assumption in most cases. We will also find it useful to use Eq. (5.7) when obtaining the acoustic/elastic transfer function since then we can model the pressure wave field of only the incident waves at the receiving transducer and use Eq. (5.7) to obtain the blocked force, without having to consider explicitly any more complex interactions of the incident waves with the receiving transducer.

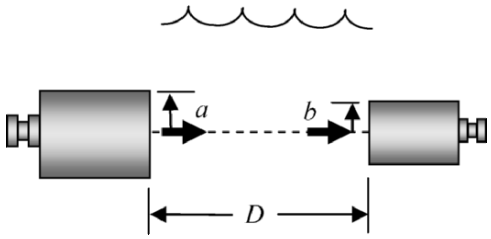

Fig. 5.4. An ultrasonic pitch-catch calibration setup where the waves generated by a circular planar piston transducer are received by a second circular planar transducer and where the transducer axes are aligned.

5.3 The Acoustic/Elastic Transfer Function

To obtain the acoustic/elastic transfer function, $t_A(\omega)$, in a general ultrasonic NDE measurement system requires a knowledge of the waves propagating in the component being inspected as well as the waves generated by any flaws present. We will develop models needed to describe those waves in Chapters 9 and 10. Here, however, we will discuss some simple setups where there are explicit analytical expressions for the acoustic/elastic transfer function. One setup that is commonly used for calibrating pitch-catch setups is shown in Fig. 5.4 where a circular planar piston transducer, of radius a, radiates waves into a fluid which are captured by a circular planar piston receiving transducer of radius b, where the two central axes of the transducers are aligned and the transducer faces are parallel to one another. In this case an explicit model has been developed for $F_{inc}(\omega)$, the force of the waves incident on the area of the receiver (in the absence of that receiver). This force is given by [5.1]

$$\begin{aligned} F_{inc}(\omega) = \rho c_p v_0(\omega) \Big\{ & \Theta \exp(ik_p D) \\ & -16a^2b^2 \int_0^{\pi/2} \frac{\sin^2 u \cos^2 u}{(a-b)^2 + 4ab\cos^2 u} \\ & \cdot \exp\left[ik_p \sqrt{D^2 + (a-b)^2 + 4ab\cos^2 u} \right] du \Big\}, \end{aligned} \tag{5.8}$$

where

$$\Theta = \begin{cases} \pi b^2 & a \geq b \\ \pi a^2 & b \geq a \end{cases} \tag{5.9}$$

and ρ, c_p are the density and compressional wave speed of the fluid, respectively, $k_p = \omega / c_p$, $v_0(\omega)$ is the velocity on the face of the transmitting transducer, and D is the distance between the transducers. If we take the acoustic radiation impedance of the transmitter as $Z_r^a = \pi a^2 \rho c_p$ and the blocked force at the receiver as $F_B = 2F_{inc}$, then we have for the transfer function

$$\begin{aligned} t_A(\omega) = \frac{2}{\pi a^2} \Big\{ & \Theta \exp(ik_p D) \\ & -16a^2 b^2 \int_0^{\pi/2} \frac{\sin^2 u \cos^2 u}{(a-b)^2 + 4ab\cos^2 u} \\ & \cdot \exp\left[ik_p \sqrt{D^2 + (a-b)^2 + 4ab\cos^2 u} \right] du \Big\}. \end{aligned} \tag{5.10}$$

In the special case when the transducers are both of the same size ($b = a$), Eq. (5.10) reduces to

$$\begin{aligned} t_A(\omega) = 2 \Big\{ & \exp(ik_p D) - \frac{4}{\pi} \\ & \cdot \int_0^{\pi/2} \sin^2 u \exp\left[ik_p \sqrt{D^2 + 4a^2 \cos^2 u} \right] du \Big\}. \end{aligned} \tag{5.11}$$

At high frequencies the integral in Eq. (5.11) can be evaluated analytically, yielding [Fundamentals]

$$\begin{aligned} t_A(\omega) = 2\exp(ikD) \Big[& 1 - \exp(ik_p a^2 / D) \\ & \cdot \left\{ J_0(k_p a^2 / D) - iJ_1(k_p a^2 / D) \right\} \Big], \end{aligned} \tag{5.12}$$

where J_0, J_1 are Bessel functions of order zero and one, respectively.

Although Eq. (5.12) is only an approximation of Eq. (5.11) it has been found to give accurate results when $k_p a >> 1$ which is well satisfied for the size of transducers and frequencies used in NDE testing. Thus, Eq. (5.12) can be regularly used in place of Eq. (5.11). This eliminates the need to numerically evaluate any integrals.

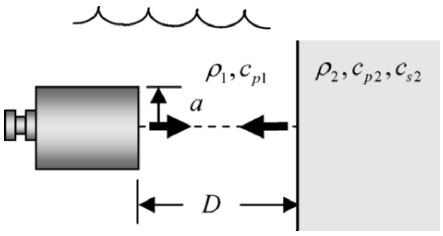

Fig. 5.5. An ultrasonic pulse-echo calibration setup where the waves generated by a circular, planar, piston transducer are reflected from a plane fluid-solid interface at normal incidence and the reflected waves are received by the same transducer.

Some more explicit results can also be obtained from Eq. (5.10) for other cases as well. For example, if we assume $a >> b$ Eq. (5.10) reduces to

$$t_A(\omega) = 2\frac{b^2}{a^2}\left\{\exp\left[ik_p D\right] - \exp\left[ik_p\sqrt{D^2 + a^2}\right]\right\}. \tag{5.13}$$

This is just the case where the receiver is small enough so that it acts as a point source and the transfer function is just proportional to the on-axis pressure of the transmitting transducer (see Chapter 8). Similarly, if we assume $b >> a$ then Eq. (5.10) becomes

$$t_A(\omega) = 2\left\{\exp\left[ik_p D\right] - \exp\left[ik_p\sqrt{D^2 + a^2}\right]\right\}, \tag{5.14}$$

which again is proportional to the on-axis pressure. For the case where the transducers are separated by a large distance D, where $D >> a$, b, Eq. (5.10) becomes

$$t_A(\omega) = -ik_p a^2 \frac{\exp\left(ik_p D\right)}{D}, \tag{5.15}$$

which has the behavior of a spherically spreading wave, a behavior that is characteristic of point sources and the transducer far-field (again, see Chapter 8).

A similar immersion calibration setup that is useful for pulse-echo testing is shown in Fig. 5.5 where a circular planar piston transducer of radius a is oriented at normal incidence to the planar surface of a solid block. In this case, the force in the waves incident on the receiver from the front face of the solid, $F_{inc}(\omega)$, can be obtained as [Fundamentals]:

$$F_{inc}(\omega) = \pi a^2 \rho_1 c_{p1} v_0(\omega) R_{12} \exp(2ik_{p1}D)\Big[1 - \exp(ik_{p1}a^2/2D) \cdot \Big\{J_0(k_{p1}a^2/2D) - iJ_1(k_{p1}a^2/2D)\Big\}\Big], \tag{5.16}$$

where ρ_1, c_{p1} are the density and compressional wave speed of the fluid, $k_{p1} = \omega / c_{p1}$ is the wave number, $v_0(\omega)$ is the velocity on the face of the transmitting transducer when it is firing, and D is the distance from the transducer to the fluid-solid interface (Fig. 5.5). The quantity R_{12} is the plane wave reflection coefficient for the interface, based on the ratio of the reflected pressure to that of the incident pressure (see appendix D) given by

$$R_{12} = \frac{\rho_2 c_{p2} - \rho_1 c_{p1}}{\rho_2 c_{p2} + \rho_1 c_{p1}}, \tag{5.17}$$

where ρ_2, c_{p2} are the density and compressional wave speed of the solid, respectively. If we again take the radiation impedance as $Z_r^a = \pi a^2 \rho_1 c_{p1}$ and the blocked force as $F_B = 2F_{inc}$, we obtain the transfer function

$$t_A(\omega) = 2R_{12} \exp(2ik_{p1}D)\Big[1 - \exp(ik_{p1}a^2/2D) \cdot \Big\{J_0(k_{p1}a^2/2D) - iJ_1(k_{p1}a^2/2D)\Big\}\Big]. \tag{5.18}$$

It is interesting to note that apart from the reflection coefficient Eq. (5.18) is identical to Eq. (5.12) if we replace the D in Eq. (5.12) by $2D$. This similarity occurs because we can view the reflected waves as arising from a fictitious "image" transmitting transducer located a distance $2D$ from the receiving transducer. Thus, for the pitch-catch response of two transducers of the same radius located co-axially in a fluid we have, from Eq. (5.12)

$$t_A(\omega) = \tilde{D}_p(k_p a^2/D)\exp(ik_p D) \tag{5.19}$$

and for the pulse-echo case, from Eq. (5.18)

$$t_A(\omega) = \tilde{D}_p(k_p a^2/2D) R_{12} \exp(2ik_p D) \tag{5.20a}$$

with

$$\tilde{D}_p(u) = 2\Big[1 - \exp(iu)\big\{J_0(u) - iJ_1(u)\big\}\Big]. \tag{5.20b}$$

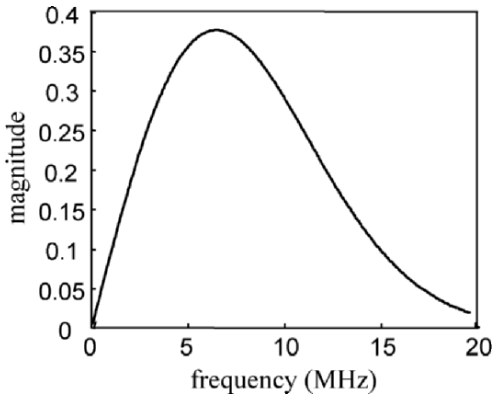

Fig. 5.6. The magnitude of the acoustic/elastic transfer function for two identical circular 3.175 mm radius planar piston transducers in water facing one another in a pitch-catch configuration as shown in Fig. 5.4 with the distance D = 444 mm. The effect of attenuation was included by using Eq. (5.22a) with the attenuation given by Eq. (5.21).

From Eq. (5.19) we can recognize the term without the $\tilde{D}_p$ function as just the transfer function for a plane wave that had traveled directly from the transmitter to the receiver, while in Eq. (5.20a) the terms without the $\tilde{D}_p$ function would be the transfer function describing a plane wave that had traveled from the transmitter to the interface, been reflected from the interface and then traveled back to the receiver. Thus, $\tilde{D}_p$ is just the diffraction correction term for these two cases that takes into account the deviations from a plane wave result. These deviations exist because the transducer produces a beam of sound rather than just a plane wave (see the discussion in Chapter 8 of diffraction corrections and the paraxial approximation). The factor of two in the $\tilde{D}_p$ expression arises simply because our transfer function is defined in terms of the blocked force rather than the force of the incident waves.

In using these transfer functions to model the propagation of waves in a real fluid, such as water, it is important to include the effects of material attenuation, which is absent in these transfer functions since they were developed under the assumption that the waves were propagating in an ideal (loss free) compressible fluid. Adding attenuation to these transfer functions can be done by including a term of the form $\exp\left[-\alpha(f)z\right]$,

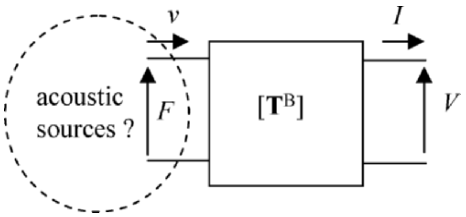

Fig. 5.7. A receiving transducer as a two port system. To use this model we need to know the nature of the acoustic sources driving the transducer.

where $\alpha(f)$ is a frequency dependent attenuation coefficient (measured in Nepers/unit length – see Appendix D) for the material the waves are traveling in and z is the distance traveled in that material. The attenuation coefficient for water at room temperature, for example, has been measured as [Fundamentals]

$$\alpha_w(f) = 25.3\times10^{-6} f^2 \text{ Nepers/mm} \tag{5.21}$$

where f is the frequency in MHz. Using this attenuation correction the transfer functions of Eq. (5.19) and (5.20) become

$$t_A(\omega) = \tilde{D}_p\left(k_p a^2 / D\right)\exp\left(ik_p D\right)\exp\left[-\alpha_w(f)D\right] \tag{5.22a}$$

and

$$t_A(\omega) = \tilde{D}_p\left(k_p a^2 / 2D\right)R_{12}\exp\left(2ik_p D\right)\exp\left[-2\alpha_w(f)D\right] \tag{5.22b}$$

An example calculation to show the behavior of the transfer function in Eq. (5.22a) is given in Fig. 5.6.

There are other simple setups where one can develop explicit expressions for the transfer function $t_A(\omega)$ but we will not discuss those cases here. The two setups we have described will be particularly useful in setting up model-based measurements that allow us to characterize all the electrical and electromechanical components in an ultrasonic measurement system (see Chapter 7) and for determining material attenuation (see Appendix D).

5.4 The Acoustic Sources and Transducer on Reception

The elements of the sound reception process are the receiving transducer, the cabling, and the receiver portion of the pulser/receiver as shown in Fig. 5.2 (a). In this section we will model the receiving transducer while in the next section we will discuss models of the cabling and receiver. By combining all of those components we will obtain the transfer function that describes the entire reception process (Fig. 5.2 (b)).

First, consider a receiving transducer *B*. We can model this transducer as a two port system where the input port is the acoustic port and the output port is the electrical port, i.e. we have reversed the inputs and outputs from the transmitting case as shown in Fig. 5.7. Note that along with this reversal we have also changed the direction of the velocity at the acoustic port and the current at the electrical port of the transducer. By inverting the transducer transfer matrix $\left[\mathbf{T}^B\right]$ that describes *B* when it is used as a transmitter (see Eq. (4.5)), using the fact that $\det\left[\mathbf{T}^B\right]=1$, and accounting for the sign changes on the velocity and current, we have

$$\begin{Bmatrix} F \\ v \end{Bmatrix} = \begin{bmatrix} T_{22}^B & T_{12}^B \\ T_{21}^B & T_{11}^B \end{bmatrix} \begin{Bmatrix} V \\ I \end{Bmatrix}, \tag{5.23}$$

i.e. the diagonal terms are interchanged but the elements of the transfer matrix in Eq. (5.23) are exactly the same elements defined for the case where the transducer acts as a transmitter. To make use of this two port system model we need to know how the force and velocity inputs are related at the acoustic port and define the "driving" sources at this port. For the receiving transducer, the "sources" at the acoustic port are obviously the waves incident on the transducer as well as the waves scattered from the transducer by the interaction of the incident waves with the transducer (see Fig. 5.8), generating a normal velocity on the face of the transducer. We will again assume that the receiving transducer behaves as a piston and let the normal velocity on its face be $v_n(\omega)$. To see how these waves generate the input force, *F*, and the input velocity, *v*, for our two port model, we break up our original problem into the sum of the two problems shown in Fig. 5.9 [5.2]. In Problem I, the face of the transducer is held rigidly fixed. In this case we have the pressure from the incident waves, p_{inc}, as well as the pressure of the waves scattered from the "blocked" transducer face, $p_{scatt}^{blocked}$. The integral of the sum of these two pressures over the transducer face is just the blocked force, $F_B(\omega)$, we

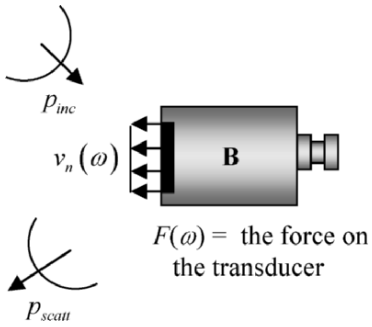

Fig. 5.8. The incident and scattered waves at a receiving transducer and the total force, $F(\omega)$, and normal velocity, $v_n(\omega)$, that those waves produce on the face of the transducer.

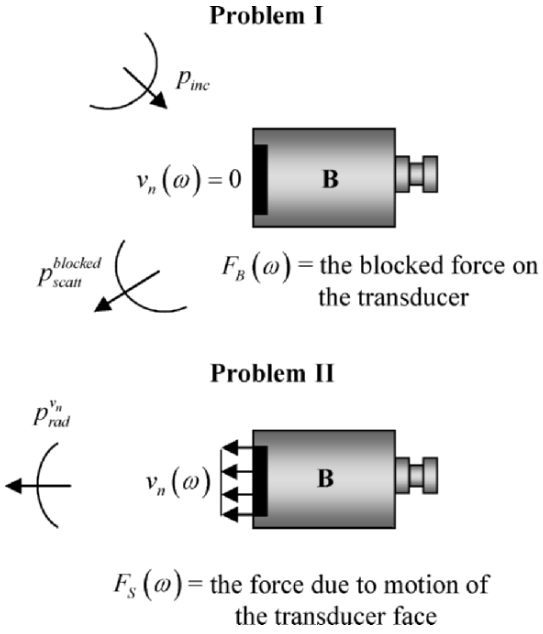

Fig. 5.9. The decomposition of the original problem shown in Fig. (5.8) into the sum of two auxiliary problems, labeled Problem I and Problem II.

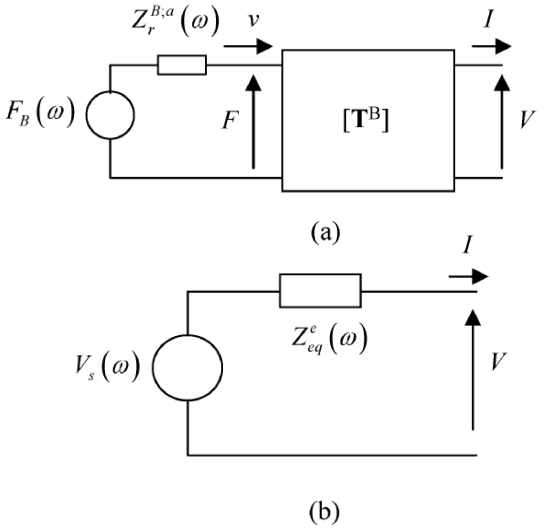

Fig. 5.10. (a) Representation of the waves received by a transducer as a blocked force source in series with the acoustic radiation impedance of the transducer, and **(b)** the representation of the acoustic sources and receiving transducer by a Thévenin equivalent voltage source and electrical impedance.

defined earlier. In Problem II the incident waves are absent and we have just the pressure of the radiated waves, $p_{rad}^{v_n}$, generated by the motion, $v_n(\omega)$, of the transducer face, which is taken as the same motion as in the original problem shown in Fig. 5.8. Let $F_s(\omega)$ be the force acting on the face of the transducer in Problem II due to this motion of the transducer face. However, Problem II is just the same form as if the transducer were radiating waves when the transducer is used as a transmitter so the force, $F_s(\omega)$, acting on the transducer in this case is related to $v_n(\omega)$ by $F_s(\omega) = Z_r^{B;a}(\omega) v_n(\omega)$, where $Z_r^{B;a}(\omega)$ is the acoustic radiation impedance of the receiving transducer *B*, the same impedance found when *B* acts as a transmitter. Since we have taken the velocity $v(\omega)$ in our two port system as flowing into the system (Fig. 5.7) and $v_n(\omega)$ is the normal velocity pointing outwards from the transducer (Fig. 5.8), we have $F_s(\omega) = -Z_r^{B;a}(\omega) v(\omega)$. The total force, $F(\omega)$, acting on the transducer, is the sum of the forces in Problems I and II, so:

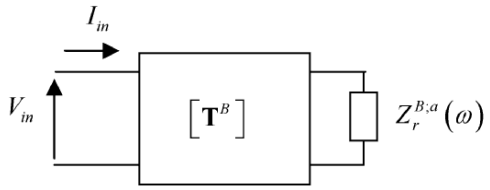

Fig. 5.11. A model of the receiving transducer when the acoustic sources are removed.

$$F(\omega) = F_B(\omega) - Z_r^{B;a}(\omega)v(\omega). \tag{5.24}$$

Equation (5.24) shows us explicitly how the force, F, and the velocity, v, are related at the acoustic port. This relationship is equivalent to the configuration shown in Fig. 5.10 (a), where a force "source", $F_B(\omega)$, is placed in series with an acoustic radiation impedance, $Z_r^{B;a}(\omega)$. Thus, we now have characterized the input side of the transducer. We see that the blocked force arises naturally in this model so that it is the quantity that makes sense to use in our transfer function definitions for both the acoustic/elastic processes and the reception process. From our previous discussion we see we could replace the blocked force source $F_B(\omega)$ by a source given by $2F_{inc}(\omega)$, where F_{inc} is the force due to the incident waves only (i.e. with the transducer absent).

Since there is at present no practical way to experimentally obtain the transfer matrix of the receiving transducer (see the discussion in Chapter 4), we need to replace the system shown in Fig. 5.10 (a) by an equivalent system whose elements we can determine. The system in Fig. 5.10 (a) is an active system (a system with a source) so Thévenin's theorem (Appendix B) allows us to replace that system with a single equivalent voltage source, $V_s(\omega)$, and an equivalent electrical impedance, $Z_{eq}^{e}(\omega)$, as shown in Fig. 5.10 (b). Recall from Appendix B that to obtain the equivalent impedance we can short out (remove) the sources and examine the ratio between the input voltage and current for this configuration. When we do that for this system we find the configuration shown in Fig. 5.11, where the transducer is simply terminated at the acoustic port by its acoustic radiation impedance, $Z_r^{B;a}(\omega)$. This configuration is

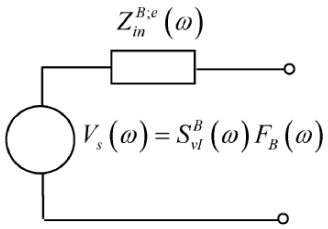

Fig. 5.12. The Thévenin equivalent circuit that characterizes a receiving transducer and its acoustic driving sources.

identical to the situation when this transducer is being used as a transmitter and so if we measured the voltage and current (V_{in}, I_{in}) shown in Fig. 5.11, we would find an equivalent impedance that is the same as that when the transducer is being used as a transmitter, i.e. $Z_{eq}^{e}(\omega) = Z_{in}^{B;e}(\omega)$ where

$$Z_{in}^{B;e}(\omega) = \frac{Z_r^{B;a} T_{11}^{B} + T_{12}^{B}}{Z_r^{B;a} T_{21}^{B} + T_{22}^{B}}. \tag{5.25}$$

To obtain the equivalent voltage source, we need to examine the system shown in Fig. 5.10 (a) under open circuit conditions. For this case, we have from Eq. (5.23)

$$\begin{aligned} F(\omega) &= T_{22}^{B}(\omega) V^{\infty}(\omega) \\ v(\omega) &= T_{21}^{B}(\omega) V^{\infty}(\omega), \end{aligned} \tag{5.26}$$

where $V^{\infty}(\omega)$ is the open circuit voltage and the source for our Thévenin equivalent circuit, i.e. $V_s(\omega) = V^{\infty}(\omega)$. Placing Eq. (5.26) into Eq. (5.24) we find

$$\frac{V^{\infty}(\omega)}{F_B(\omega)} = \frac{1}{T_{22}^{B}(\omega) + Z_r^{B;a}(\omega) T_{21}^{B}(\omega)}. \tag{5.27}$$

This ratio is a receiving sensitivity called the open-circuit, blocked force receiving sensitivity, $M_{VF_B}^{B;\infty}(\omega)$ [5.3]. However, comparing Eq. (5.27) with Eq. (4.20) where we defined the sensitivity, $S_{vI}^{B}(\omega)$, for this transducer when used as a transmitter, we see that:

$$M_{VF_B}^{B;\infty}(\omega) = S_{vI}^{B}(\omega) \tag{5.28}$$

and it follows that the Thévenin equivalent voltage is just

$$V_s(\omega) = S_{vI}^{B}(\omega) F_B(\omega), \tag{5.29}$$

which reduces the transducer and its driving sources to the simple circuit shown in Fig. 5.12. Since in Chapter 7 we will show that it is possible to obtain S_{vI}^{B} and $Z_{in}^{B;e}$ by purely electrical measurements, those measurements will determine completely the role of the transducer when acting as both a transmitter and receiver of sound.

The equality of the two sensitivities in Eq. (5.28) is not accidental. In fact, it is directly a consequence of the fact that the transducer is assumed to be a reciprocal device. Thus, Eq. (5.28) can be considered as a statement of *transducer reciprocity* (see [5.5] for further discussions of transducer reciprocity). This fact can be easily demonstrated by again starting from the transfer matrix of a transducer *B* when it is acting as a transmitter (Eq. (4.5)) and then obtaining the transfer matrix relationship of Eq. (5.23) but without assuming that the transducer is reciprocal (i.e. let $\det\left[\mathbf{T}^B\right] \neq 1$). In place of Eq. (5.23) we then find during reception that

$$\begin{Bmatrix} F \\ v \end{Bmatrix} = \frac{1}{\det\left[\mathbf{T}^B\right]} \begin{bmatrix} T_{22}^B & T_{12}^B \\ T_{21}^B & T_{11}^B \end{bmatrix} \begin{Bmatrix} V \\ I \end{Bmatrix}. \tag{5.30}$$

Thus, when we relate the force and velocity in Eq. (5.30) to the open-circuit receiving voltage, V^{∞}, in place of Eq. (5.26) we obtain

$$\begin{aligned} F(\omega) &= T_{22}^B(\omega) V^{\infty}(\omega) / \det\left[\mathbf{T}^B\right] \\ v(\omega) &= T_{21}^B(\omega) V^{\infty}(\omega) / \det\left[\mathbf{T}^B\right], \end{aligned} \tag{5.31}$$

which, when placed into Eq. (5.24), gives

$$\begin{aligned} M_{VF_B}^{B;\infty} &= \frac{V^{\infty}(\omega)}{F_B(\omega)} = \frac{\det\left[\mathbf{T}^B\right]}{T_{22}^B(\omega) + Z_r^{B;a}(\omega) T_{21}^B(\omega)} \\ &= \det\left[\mathbf{T}^B\right] S_{vI}^B, \end{aligned} \tag{5.32}$$

where we have also used the definition of the transmitting sensitivity S_{vI}^{B} given by Eq. (4.20). Equation (5.32) shows that the equality of the two

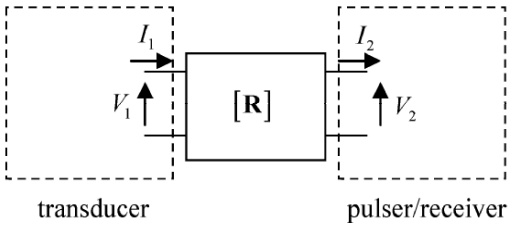

Fig. 5.13. A two port model of the receiving cable.

sensitivities as stated by Eq. (5.28) is then equivalent to requiring $\det\left[\mathbf{T}^B\right]=1$, i.e. the transducer must be reciprocal.

5.5 The Cable and the Receiver in the Reception Process

The role of the cable in the reception process is exactly the same as its role in the sound generation process. We can characterize the cable by a 2x2 reciprocal transfer matrix, $[\mathbf{R}]$, where (see Fig. 5.13)

$$\begin{Bmatrix} V_1 \\ I_1 \end{Bmatrix} = \begin{bmatrix} R_{11} & R_{12} \\ R_{21} & R_{22} \end{bmatrix} \begin{Bmatrix} V_2 \\ I_2 \end{Bmatrix} \tag{5.33}$$

and the reversing of the current directions does not affect this relationship if the cable is reciprocal ($\det[\mathbf{R}]=1$) and $R_{11}=R_{22}$ as found in a transmission line model of the cable. If the cable does not exactly satisfy these requirements of the transmission line model then we can take such behavior into account by replacing Eq. (5.33) by

$$\begin{Bmatrix} V_1 \\ I_1 \end{Bmatrix} = \frac{1}{\det[\mathbf{R}]} \begin{bmatrix} R_{22} & R_{12} \\ R_{21} & R_{11} \end{bmatrix} \begin{Bmatrix} V_2 \\ I_2 \end{Bmatrix}, \tag{5.34}$$

where $(R_{11}, R_{12}, R_{21}, R_{22})$ are the measured transfer matrix of the cable when it is transferring signals from the pulser/receiver to the transducer during the sound generation process. These components of the receiving cable transfer matrix can again be found through the electrical measurements described in Chapter 3.

The receiver part of a pulser/receiver amplifies the received signals and can also filter them. Figure 2.1 shows these types of controls on the

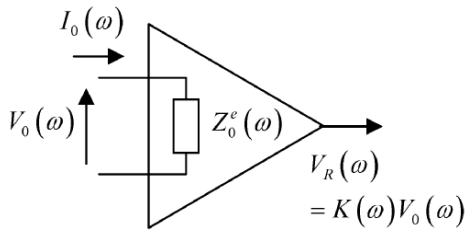

Fig. 5.14. Model of a receiver as an electrical impedance and an amplification factor.

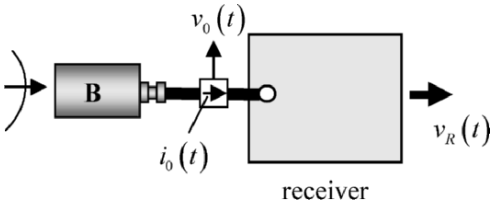

Fig. 5.15. A measurement setup where the waves driving a receiving transducer are used as inputs to the receiver. The input voltage, $v_0(t)$, and current, $i_0(t)$, are measured at the input port of the receiver, as is the receiver output voltage, $v_R(t)$.

right side of the front panel of a spike pulser and Fig. 2.4 shows similar gain and filtering settings that can be made on under computer control of a square wave pulser. Here, any filtering operations of the receiver will not be modeled as they can be easily applied to the unfiltered output at a later stage if desired. In many quantitative studies filtering may be detrimental because it removes frequency components that may contain useful information.

Since the receiver provides an electrical termination at one end of the cable, we will model the receiver as an electrical impedance, $Z_0^e(\omega)$ (Fig. 5.14). The amplifier action of the receiver will be modeled by an amplification (gain) factor, $K(\omega) = V_R(\omega)/V_0(\omega)$, as shown in Fig. 5.14, where $V_R(\omega)$ is the output voltage frequency components of the receiver and $V_0(\omega)$ is the corresponding voltage at the receiver's input port. By measuring the voltages and currents at the input and output of the receiver when it is receiving signals from a receiving transducer (see Fig. 5.15)

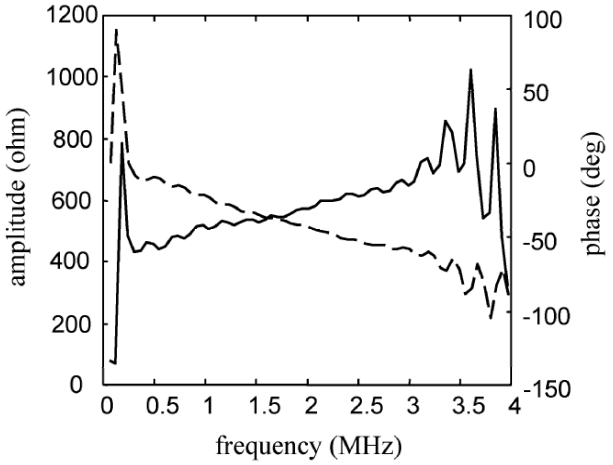

Fig. 5.16. The measured magnitude (solid line) and phase (dashed line) of the electrical impedance, $Z_0^e(\omega)$, of the receiver portion of a Panametrics 5052PR pulser/receiver when driven by a 2.25 MHz transducer in a pitch-catch mode.

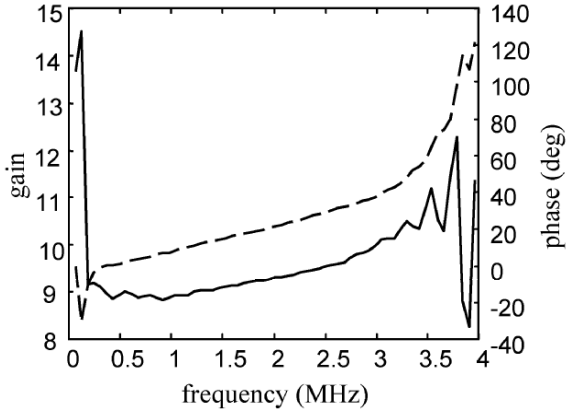

Fig. 5.17. The measured magnitude (solid line) and phase (dashed line) of the amplification (gain) factor, $K(\omega)$, of the receiver portion of a Panametrics 5052PR pulser/receiver when driven by a 2.25 MHz transducer in a pitch-catch mode.

and calculating their Fourier transforms, the quantities $V_0(\omega)$, $I_0(\omega), V_R(\omega)$ can be found for a specific gain setting of the receiver. From these measurements both the impedance, $Z_0^e(\omega)$, and the amplification factor, $K(\omega)$, can be obtained since

$$Z_0^e(\omega) = \frac{V_0(\omega)}{I_0(\omega)}$$
$$K(\omega) = \frac{V_R(\omega)}{V_0(\omega)}, \tag{5.35}$$

where a Wiener filter can be used to desensitize these divisions to noise (see Appendix C). Figure 5.16 shows the measured impedance of a Panametrics 5052PR pulser/receiver determined in this fashion when the pulser/receiver is operating in a pitch-catch mode. Fig. 5.17 gives the corresponding measured amplification (gain) factor. There is little structure seen in the impedance plot as a function of frequency. It is nearly a constant, having a value of approximately 500 ohms. This is consistent with the circuit diagrams of this particular instrument in a pitch-catch mode. The amplification factor also has little structure, having a value near 10 which corresponds well with the 20dB gain setting at which the measurements were taken. Since the 2.25 MHz receiving transducer used in these measurements band limits the received response the results shown in Figs. 5.16 and 5.17 can only be reliably estimated over the bandwidth present. If the transducer used in such a calibration is the same as the one used in an actual inspection, this may not be an issue since the same bandwidth constraints will also be present in the inspection. Otherwise, we may need to excite the receiver with a wider bandwidth source or combine the measurements made with several different transducers to obtain $Z_0(\omega), K(\omega)$ over a larger range of frequencies.

In a pulse-echo mode the received signals must pass through some of the circuits of the pulser section so it is not surprising that in this case the properties of the receiver are affected by the pulser settings. Figure 5.18 (a) shows the behavior of the amplification factor, $K(\omega)$, of a spike pulser/receiver computed at two different damping settings and Fig. 5.18 (b) gives the receiving impedance, $Z_0^e(\omega)$, as measured over a range of different damping settings. The receiver was driven in these cases by waves received from a broadband 5 MHz transducer in a pulse-echo setup of the type shown in Fig. 5.5.

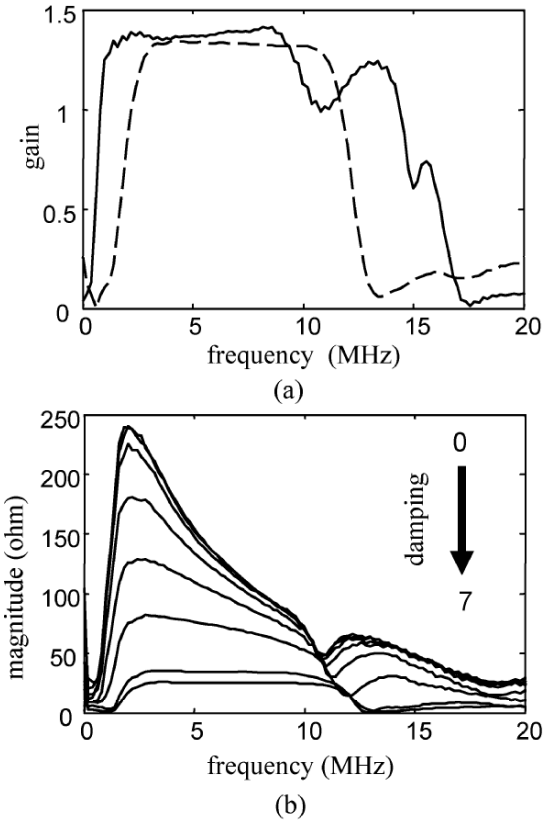

Fig. 5.18. (a) Magnitude of the amplification factor for the receiver section of a spike pulser/receiver in a pulse-echo mode obtained at a damping setting of 2 (solid line) and a damping setting of 9 (dashed line). **(b)** The equivalent impedance of the spike pulser/receiver at a range of damping settings from 0 to 7 (the arrow indicates the trend of the curves for changing damping settings).

Figure 5.19 shows the results of measurement of the amplification factor and receiving impedance of a square wave pulser/receiver when operated in a pitch-catch mode while Fig. 5.20 shows these same parameters when the square wave pulser is operated in a pulse-echo mode. In both cases the receiver was being driven by a broadband 5 MHz transducer. In the pulse-echo mode it can be seen that there is some dependency of the square wave receiver parameters on the pulse width setting in pulse-echo but these changes are not large.

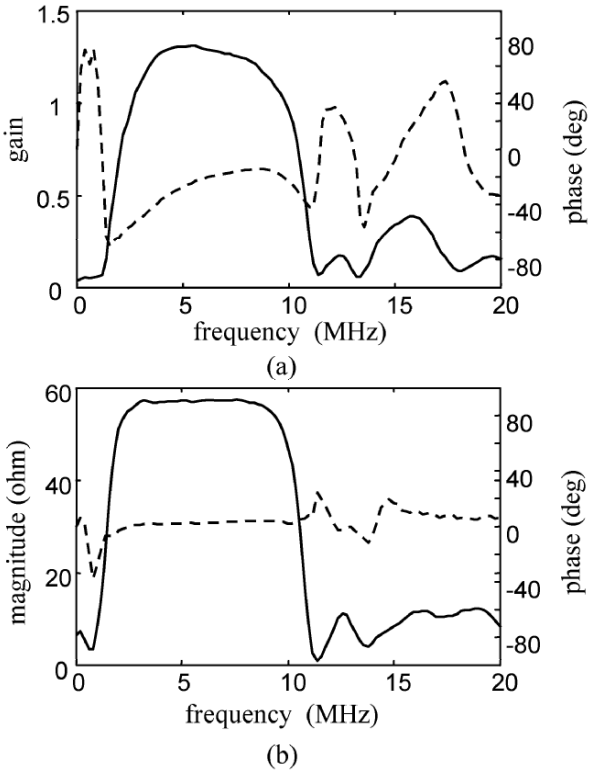

Fig. 5.19. (a) The magnitude (solid line) and phase (dashed line) of the amplification (gain) factor of the receiver section of a square wave pulser/receiver in a pitch-catch mode. **(b)** The magnitude and phase of the equivalent impedance of the receiver section of a square wave pulser/receiver in a pitch-catch mode.

5.6 A Complete Reception Process Model

By combining our transducer, cabling and receiver models we have the complete reception process shown in Fig. 5.21. From Fig. 5.21 we have

$$S_{vI}^{B} F_B - V_2 = Z_{in}^{B;e} I_2 \tag{5.36}$$

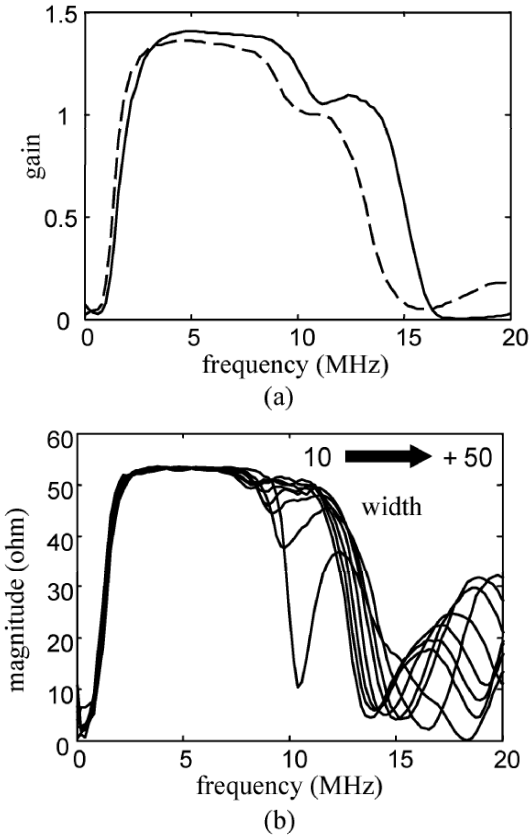

Fig. 5.20. (a) The magnitude of the amplification factor of the receiver section of a square wave pulser/receiver in a pulse-echo mode obtained at a pulse width setting of 10 (solid line) and a pulse width setting of 50 (dashed line). **(b)** The magnitude of the receiving impedance of the receiver section of a square wave pulser/receiver in a pulse-echo mode for a range of pulse width settings (the arrow indicates the trend of the curves for changing pulse widths).

$$\begin{Bmatrix} V_2 \\ I_2 \end{Bmatrix} = \begin{bmatrix} R_{22} & R_{12} \\ R_{21} & R_{11} \end{bmatrix} \begin{Bmatrix} V_0 \\ I_0 \end{Bmatrix} \tag{5.37}$$

$$V_R = K V_0 \tag{5.38}$$

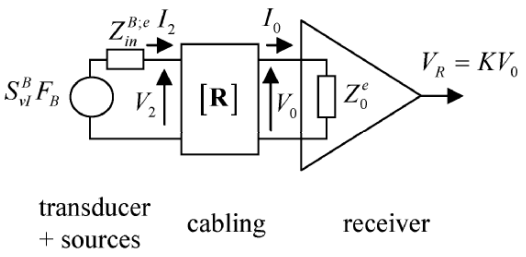

Fig. 5.21. A model of the entire sound reception process.

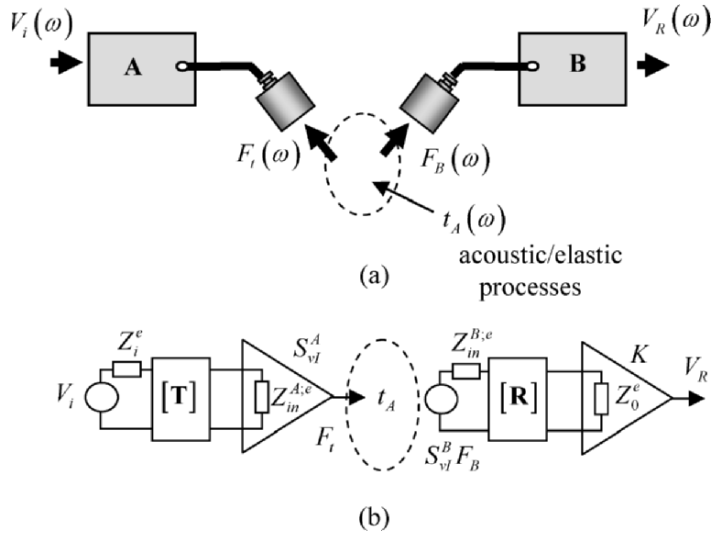

Fig. 5.22. (a) All the electrical and electromechanical elements of both the sound generation and sound reception parts of an ultrasonic measurement system, and **(b)** their representation by equivalent sources, impedances, sensitivities, amplification factors, and transfer matrix elements. All the wave propagation and scattering processes are shown in terms of the acoustic/elastic transfer function, $t_A(\omega)$.

$$V_0 = Z_0^e I_0, \tag{5.39}$$

where the components of the cabling transfer matrix are those obtained considering (V_0, I_0) as the input side of the cabling and we have assumed $\det[\mathbf{R}] = 1$ (i.e. the cable is reciprocal) but have not assumed that $R_{11} = R_{22}$ (see the discussion leading to Eq. (5.34)). Using Eqs. (5.36 - 5.39) it is easy to show that the transfer function for this entire reception process, $t_R(\omega)$, is given by [5.4]

$$t_R(\omega) = \frac{V_R(\omega)}{F_B(\omega)} = \frac{K Z_o^e S_{vI}^B}{\left(Z_{in}^{B;e} R_{11} + R_{12}\right) + \left(Z_{in}^{B;e} R_{21} + R_{22}\right) Z_o^e} \tag{5.40}$$

in terms of all the parameters defined earlier. Recall the transfer function for the sound generation process, $t_G(\omega)$, was given by Eq. (4.21) as

$$t_G(\omega) = \frac{F_t(\omega)}{V_i(\omega)} = \frac{Z_r^{A;a} S_{vI}^A}{\left(Z_{in}^{A;e} T_{11} + T_{12}\right) + \left(Z_{in}^{A;e} T_{21} + T_{22}\right) Z_i^e}. \tag{5.41}$$

All the electrical and electromechanical components in an ultrasonic measurement system are shown in Fig. 5.22 (a). The corresponding models are shown in Fig. 5.22 (b). It can be seen from Fig. 5.22 (b) that both the complex sound generation and reception processes models are combined in very similar ways, reflecting the close similarity between the sound generation and receptions transfer functions in Eqs. (5.40) and (5.41). Figure 5.23 shows an example where the magnitude and phase of a sound reception transfer function, $t_R(\omega)$, was experimentally determined by characterizing all the components contained in Eq. (5.40). In this case the receiver was the receiver section of a Panametrics 5052 PR pulser/receiver (measured at a specific gain setting). The cabling consisted of 1.83 m of flexible 50 ohm coaxial cable connected to a 0.76 m fixture rod. The rod also contained internal cabling and was terminated by a right-angle adapter to which the transducer was connected. The transducer was a relatively broadband 6.35 mm diameter, 5 MHz immersion transducer. The sensitivity and impedance of the transducer were obtained by the methods which will be discussed in Chapter 6.

In Chapter 7 it will be shown that these sound generation and reception transfer functions can be combined with the pulser voltage

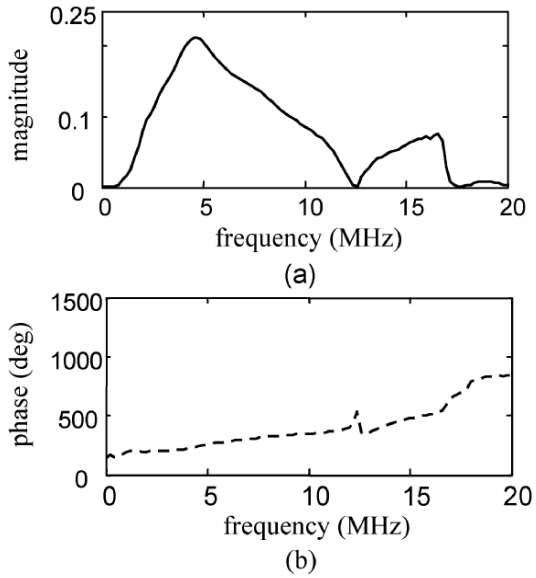

Fig. 5.23. A sound reception transfer function obtained experimentally. **(a)** Magnitude versus frequency and **(b)** phase versus frequency.

source term, $V_i(\omega)$, to form what is called the system function. It will also be shown in that Chapter that the system function can be obtained either by measuring of all its electrical and electromechanical components or by performing a single voltage measurement in a calibration setup. Thus, the acoustic/elastic transfer function, $t_A(\omega)$, shown in Fig. 5.22 is the only remaining part of the ultrasonic measurement system that is needed to completely characterize an entire ultrasonic measurement system. Since this acoustic/elastic transfer function involves the wave fields inside of solid components that are being inspected, it is not practical to measure this transfer function experimentally. Instead, accurate beam models and flaw scattering models are needed to describe $t_A(\omega)$ for an ultrasonic flaw measurement system. In Chapters 8-10 such ultrasonic beam models and flaw scattering models will be described in detail. In Chapter 11 these beam models and scattering models will be combined with a general reciprocity relationship to obtain the acoustic/elastic transfer function for many ultrasonic flaw measurement setups.

5.7 References

5.1 Beissner K (1981) Exact integral expression for the diffraction loss of a circular piston. Acustica 19: 21-217
5.2 Dang CJ, Schmerr LW, Sedov A (2002) Modeling and measuring all the elements of an ultrasonic nondestructive evaluation system. I: Modeling foundations. Research in Nondestructive Evaluation 14: 141-176
5.3 Dang CJ, Schmerr LW, Sedov A (2002) Ultrasonic transducer sensitivity and model-based transducer characterization. Research in Nondestructive Evaluation 14: 203-228
5.4 Dang CJ, Schmerr LW, Sedov A (2002) Modeling and measuring all the elements of an ultrasonic nondestructive evaluation system. II: Model-based measurements. Research in Nondestructive Evaluation 14: 177-201
5.5 Auld BA (1990) Acoustic fields and waves in solids, 2nd ed., Vols. 1, 2. Krieger Publishing Co., Malabar, FL

5.8 Exercises

1. Using Eqs. (5.21) and (5.22b) write a MATLAB function t_a that computes the acoustic/elastic transfer function for the pulse-echo setup shown in Fig. 5.5, where the fluid is water at room temperature. The calling sequence for this function should be:

```
>> t =t_a(f, a, d, d1, d2,c1,c2);
```

where f is the frequency (in MHz), a is the radius of the transducer (in mm), d is the distance from the transducer to the plane surface (in mm), d1 is the density of the fluid (in gm/cm^3), c1 is the compressional wave speed of the fluid (in m/sec), d2 is the density of the solid (in gm/cm^3), and c2 is the compressional wave speed of the solid (in m/sec).

Using this function, obtain a plot of the magnitude of this transfer function versus frequency similar to Fig. 5.6 for a = 6.35 mm, d = 100 mm, d1 = 1.0 gm/cm^3, c1 = 1480 m/sec, d2 = 7.9 gm/cm^3, c2 = 5900 m/sec (steel). Let the frequencies range from 0 to 20 MHz. On the same plot, show the magnitude of this transfer function versus frequency when the attenuation of the fluid is neglected, so that the effects of attenuation on this function can be demonstrated.